



OPEN

The hemopexin domain of matrix metalloproteinase-9 attenuates lipopolysaccharide-induced interleukin-6 secretion in liver

Yen-Ting Chien^{1,3}, Yu-Hsiang Liao^{1,2,3}, Xian Wei Chong¹, Meng-Chieh Hsu¹, Chih-Hsien Chiu¹ & Chien Huang¹✉

Matrix metalloproteinase-9 (MMP-9) has been implicated in modulating hepatic inflammation, as MMP-9 deficiency exacerbates liver damage and inflammatory responses in sepsis models. However, the mechanisms underlying its anti-inflammatory properties, particularly in the context of lipopolysaccharide (LPS) induced liver inflammation, remain poorly understood. Plasma and liver cytokine levels in MMP-9 catalytic-deficient mice were measured after the administration of 4.5 mg/kg LPS injections for 4 and 24 h. LPS-induced inflammatory responses were examined in mouse primary hepatocytes, hepatic, and macrophage cell lines by analyzing the secretion and expression of interleukin-6 (IL-6) in the gain- and loss-of-function of MMP-9. *In vitro* models were established by lentiviral infection, including MMP-9 knockout, Tet-On inducible wild-type MMP-9, and MMP-9 with catalytic domain mutation or hemopexin (PEX) domain deletion in wild-type parent cells. Following LPS treatment, MMP-9 catalytic-deficient mice demonstrated a significant increase in IL-6 levels, along with a notable decrease in MMP-9 protein expression relative to wild-type mice, in both plasma and liver tissue. Overexpression of MMP-9 significantly attenuated LPS-induced IL-6 secretion in hepatocytes. Notably, even the overexpression of a catalytically inactive MMP-9 mutant retained this suppressive effect. In contrast, deletion of the PEX domain abolished the inhibitory effect of MMP-9 on IL-6 secretion, indicating that the PEX domain, rather than its catalytic activity, is essential for this regulatory function. Moreover, MMP-9 overexpression markedly suppressed IL-6 secretion in response to LPS stimulation, whereas its genetic deletion significantly enhanced IL-6 secretion in macrophages. This study demonstrated that MMP-9 could partially protect the liver from LPS-induced damage by decreasing pro-inflammatory cytokine levels via its PEX domain, indicating the anti-inflammatory potential of the MMP-9 PEX domain against endotoxin.

Keywords Hepatology, Inflammation, Endotoxin, pro-inflammatory cytokine, Macrophages

Abbreviations

MMP-9	Matrix metalloproteinase-9
PEX domain	Hemopexin domain
LPS	Lipopolysaccharide
IL-6	Interleukin 6
TNF α	Tumor Necrosis Factor- α
KO	Knockout
WT	Wild-type
Dox	Doxycycline
TO	Tet-on

Lipopolysaccharide (LPS), a major component of the outer membrane of gram-negative bacteria, serves as a potent activator of the innate immune system by triggering Toll-like receptor 4 (TLR4) signaling¹. As an endotoxin,

¹Laboratory of Animal Physiology, Department of Animal Science and Technology, National Taiwan University, 50, Lane 155, Sec 3, Keelung Rd., 106, Taipei 101617, Taiwan. ²Department of Animal Science, Cornell University, Ithaca, NY 14853, USA. ³Yen-Ting Chien and Yu-Hsiang Liao contributed equally to this work. ✉email: chienhuang@ntu.edu.tw

LPS plays a crucial role in activating the innate immune system by initiating a cascade of pro-inflammatory responses that are essential for the defense against infections. However, once infection and inflammation become dysregulated, it can trigger an excessive immune response, which leads to systemic inflammation and potentially results in septic shock, eventually leading to life-threatening multi-organ failure². The liver plays a central role in both innate and adaptive immunity, and serves as a critical site for pathogen clearance and immune modulation³. Upon infection, pathogens and pro-inflammatory cytokines from peripheral sites enter the liver via the portal circulation^{4,5}. These stimulations lead Kupffer cells to secrete several pro-inflammatory cytokines, such as interleukin-6 (IL-6) and tumor necrosis factor-alpha (TNF- α)⁶. These cytokines activate hepatocytes to secrete acute-phase proteins, including C-reactive protein (CRP), complement factors, and serum amyloid A (SAA)⁷. Kupffer cells, the liver's resident macrophages, maintain hepatic immune homeostasis⁸. Kupffer cells and hepatocytes both express TLR4, allowing them to respond to LPS stimulation and contribute to the hepatic inflammatory response through IL-6 secretion^{9–11}. Consequently, both cells are integral components of the hepatic innate immune response, coordinating the inflammatory cascade that is critical for the resolution of infection but also potentially contributing to pathological outcomes in cases of immune dysregulation^{12,13}.

In addition to pro-inflammatory cytokines, LPS upregulates immune-regulatory genes, including matrix metalloproteinase-9 (MMP-9), a proteolytic enzyme that degrades components of the extracellular matrix (ECM)^{14,15}. MMP-9 is primarily recognized for its ability to cleave type IV and V collagens¹⁶. Beyond ECM degradation, MMP-9 plays a crucial role in tissue remodeling processes, including wound healing, angiogenesis, immune responses, and immune cell migration^{17–21}. Its activation is tightly regulated through a cascade of proteolytic events²², and its enzymatic activity is counterbalanced by endogenous inhibitors such as tissue inhibitor of metalloproteinases-1 (TIMP-1)²³. Beyond ECM remodeling, MMP-9 also regulates multiple signaling pathways by cleaving bioactive proteins²⁴. Functionally, MMP-9 exhibits both catalytic activity and non-catalytic roles mediated by its hemopexin (PEX) domain. The catalytic domain governs the proteolysis of ECM components and bioactive substrates^{24,25}. In contrast, the PEX domain mediates protein–protein interactions and receptor engagement, contributing to cell signaling and migration independent of enzymatic activity^{26,27}. These distinct functions show that MMP-9 plays a wide range of roles in both physiological and pathological processes.

According to single-cell RNA sequencing data from the public liver dataset²⁸, neutrophils exhibit the highest levels of *Mmp9* expression, but they represent only a relatively small proportion of the liver population. Kupffer cells, which account for approximately 10–15% of liver cells²⁹, display moderate to high *Mmp9* expression, underscoring their substantial contribution to the hepatic MMP-9 reservoir. Hepatocytes, although characterized by comparatively low *Mmp9* expression, comprise 60–70% of all liver cells^{30,31}, suggesting that even modest expression levels in hepatocytes may have a significant functional impact. Collectively, this study supports the use of hepatocytes and liver-resident macrophages as biologically relevant *in vitro* models for investigating MMP-9-mediated processes in hepatic physiology.

Several studies have shown that MMP-9 has an anti-inflammatory potential^{32–35}. A previous study reported that MMP-9 knockout (KO) mice have less tolerance to *E. coli*-induced peritonitis and greater levels of serum pro-inflammatory cytokines than wild-type (WT) mice³⁶. A recent study found that MMP-9 knockdown increased the gene and protein expression of LPS-induced pro-inflammatory cytokines, including interleukin 1-beta (IL-1 β) and TNF- α . Moreover, MMP-9 overexpression reduces the expression of IL-1 β and TNF- α in mouse osteoblasts³³. However, the mechanism by which MMP-9 regulates hepatic pro-inflammatory cytokines remains unclear. Therefore, this study aimed to investigate whether MMP-9 protects the liver against LPS-induced inflammation and elucidate the underlying mechanisms.

Results

MMP-9 deficiency aggravates LPS-induced systemic inflammation and liver damage in mice

To investigate the role of MMP-9 in hepatic inflammatory responses, MMP-9-deficient (MMP-9 KO) mice were administered either 4.5 mg/kg LPS or saline for 4 and 24 h, as shown in Fig. 1A. These genetically modified mice carried a targeted deletion in the MMP-9 gene, in which a portion of exon 2 and the entire intron 2 were replaced by a neo-PGK cassette, as previously described³⁷. Despite retaining MMP-9 protein expression, MMP-9 KO mice lacked enzymatic function, whereas other functional domains remained structurally intact.

Serum biochemistry analysis was performed to assess systemic inflammation following LPS administration (Table 1). Alanine aminotransferase (ALT) levels, a well-established biomarker of hepatocellular damage, were significantly elevated in the LPS-exposed group compared to the saline-treated controls in MMP-9 KO mice, indicating hepatic injury. Additionally, aspartate aminotransferase (AST) and lactate dehydrogenase (LDH), both nonspecific indicators of tissue injury, were markedly increased in the LPS-exposed group compared to the saline-treated controls in MMP-9 KO mice, suggesting exacerbated systemic inflammation after LPS exposure due to MMP-9 deficiency. In addition, plasma IL-6 levels were significantly elevated in MMP-9 KO mice compared with WT mice at 4 and 24 h following LPS injection. In contrast, a significant increase in plasma TNF- α levels was observed in KO mice relative to WT mice exclusively at 24 h after LPS administration (Fig. 1B, C), indicating a sustained and enhanced systemic inflammatory response in the absence of MMP-9.

Histological examination of liver sections stained with hematoxylin and eosin revealed preserved hepatic architecture in the saline-treated controls, whereas LPS-treated mice exhibited marked immune cell infiltration (Fig. 1D, black arrows), which may reflect underlying inflammatory processes. However, the immunohistochemistry using F4/80, a macrophage-specific marker, revealed no significant differences in the F4/80-positive areas in the hepatic sinusoids between LPS-treated WT and KO mice (Fig. 1E), suggesting that MMP-9 deficiency does not affect macrophage recruitment during the acute phase of inflammation.

The hepatic MMP-9 expression and enzymatic activity were also assessed. Consistent with previous studies³⁸, LPS treatment induced MMP-9 activity in WT mice but not in KO mice (Fig. 1F). In addition, mutated MMP-

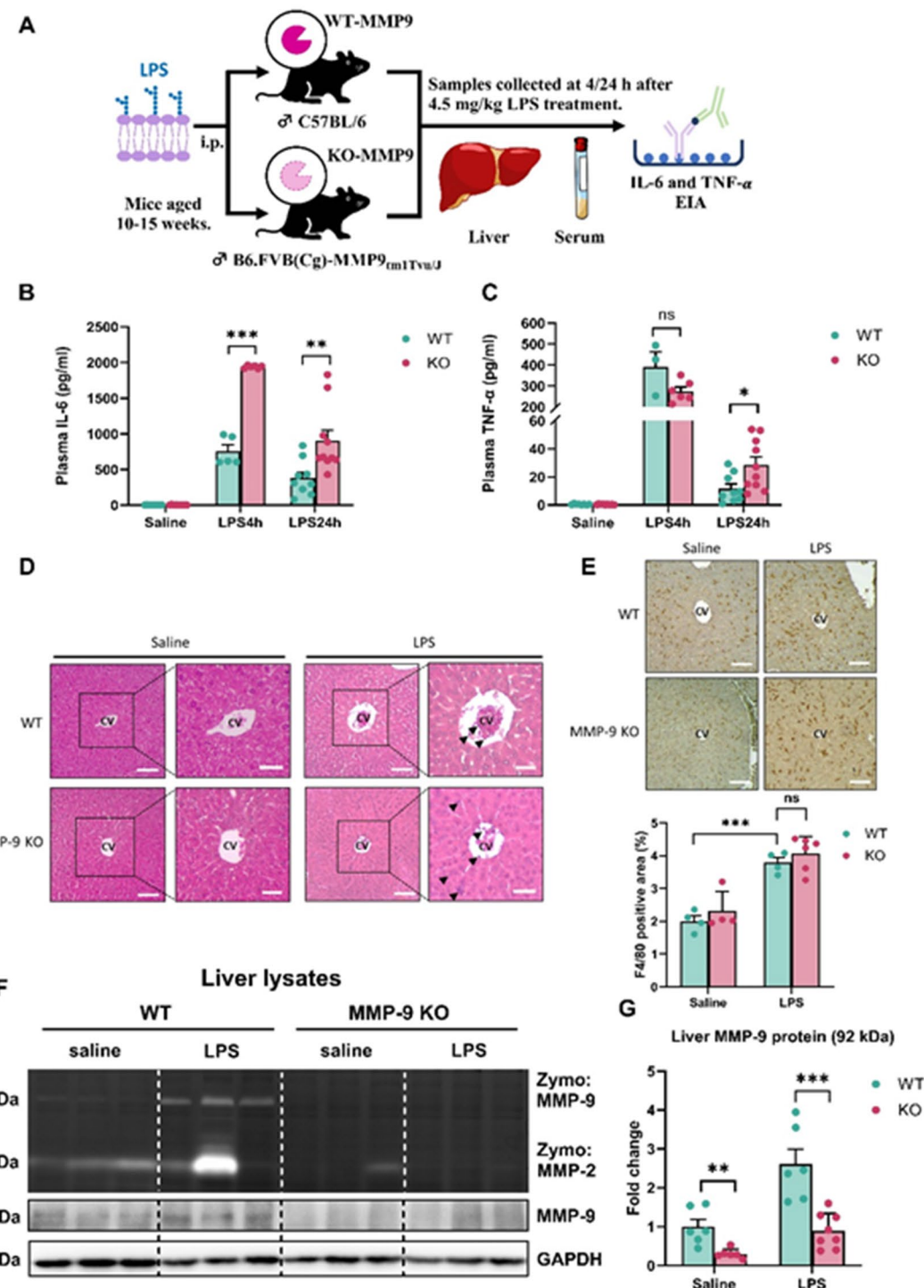


Fig. 1. MMP-9 knockout enhances systemic inflammatory response after LPS administration. (A) Schematic overview of the *in vivo* experimental workflow. WT and MMP-9 KO mice received intraperitoneal LPS injections (4.5 mg/kg) for either 4–24 h. (B, C) Plasma concentrations of IL-6 and TNF- α were measured at the indicated time points. (D) Representative hematoxylin and eosin (H&E)-stained liver sections from each group. Central vein (CV) and immune cell infiltration (black arrow) are indicated. Scale bar = 100 μ m. (E) Immunohistochemical staining of F4/80 in liver tissue. CV denotes the central vein. Quantification of F4/80-positive area is shown. Scale bar = 100 μ m. (F) Representative zymography and immunoblotting of MMP-9 enzyme activity and protein expression in total liver lysates. (G) Densitometric analysis of mutated MMP-9 expression normalized to GAPDH. All LPS treatments were performed for 24 h unless otherwise specified. Data are presented as mean \pm SEM ($n = 4$ –8 per group). Statistical comparisons were performed using unpaired t-tests. * $P < 0.05$, ** $P < 0.01$, *** $P < 0.001$ vs. WT + LPS; ns: not significant.

	LDH (IU/L)	GPT/ALT (IU/L)	GOT/AST (IU/L)	Alb (g/dL)
WT Saline	2,118 ± 429	61.7 ± 42.7	258.0 ± 148.3	2.38 ± 0.15
WT LPS	2,647 ± 524	139.6 ± 70.6	374.8 ± 62.3	1.90 ± 0.07 ^{&&}
KO Saline	2,098 ± 852	57.2 ± 33.8	279.3 ± 124.4	2.42 ± 0.19
KO LPS	3,721 ± 337 ^{&&, #}	221.0 ± 148.5 [‡]	545.9 ± 225.7 [‡]	1.89 ± 0.16 ^{&&}

Table 1. Blood biochemistry of WT and MMP-9 KO mice after LPS administration. LDH: Lactic dehydrogenase, ALT: Alanine aminotransferase, AST: Aspartate aminotransferase, Alb: Albumin. WT and MMP-9 KO mice were injected with saline or 4.5 mg/kg LPS for 24 h. Data are shown as mean ± SD. $n=3-7$. Statistical comparisons were conducted using Student's t-test. $\& p < 0.05$, $\&\& p < 0.01$, compared to saline group; $\# p < 0.05$, $\#\# p < 0.01$, compared to WT group.

9 protein expression was significantly reduced in KO mice following LPS treatment compared to WT controls (Fig. 1F, G), suggesting a feedback mechanism regulating the expression during inflammation. Collectively, these findings indicated that MMP-9 deficiency exacerbates LPS-induced systemic inflammation and hepatic injury, whereas macrophage recruitment in the liver remains unaffected.

MMP-9 deficiency aggravates LPS-induced pro-inflammatory cytokines in the liver

LPS stimulation triggers a robust pro-inflammatory cytokine response in both the systemic circulation and liver tissue³⁹. Consistent with the plasma data, hepatic IL-6 protein expression was significantly higher in MMP-9 KO mice than in WT mice only at 24 h (Fig. 2A). In contrast, TNF- α protein expression in the liver was comparable between the two groups (Fig. 2B).

Transcriptional analysis further revealed that MMP-9 deficiency selectively enhanced the hepatic expression of *Il6* mRNA, while *Tnf* and *Il1b* gene expression remained unaffected under LPS stimulation (Fig. 2C-E). Notably, MMP-9 deficiency also led to the upregulation of pattern recognition receptors and co-stimulatory molecules associated with LPS signaling, including *Thr4* and *Cd14* (Fig. 2F, G). Nuclear factor kappa B (NF- κ B) is a central transcription factor downstream of LPS-mediated signaling and an upstream regulator of both IL-6 and MMP-9 expression^{38,40,41}. The hepatic protein level of NF- κ B was markedly elevated in the LPS-treated groups, and significantly higher expression was observed in MMP-9 KO mice (Fig. 2H, I). This suggests that the absence of MMP-9 enhances NF- κ B activation, thereby amplifying the pro-inflammatory signaling pathways in the liver.

Overall, these findings demonstrate that MMP-9 deficiency exacerbates LPS-induced hepatic inflammatory response, primarily through the upregulation of IL-6 and enhanced NF- κ B signaling, without uniformly affecting other cytokine pathways. However, the precise mechanism by which MMP-9 deficiency augments innate immune activation remains unclear. In the *in vivo* system, the complexity of physiological conditions makes it difficult to clarify the underlying molecular mechanisms. Nevertheless, it provides an important insight, suggesting that the loss of enzymatic activity or the diminished protein expression of MMP-9 (Fig. 1G) may contribute to this process.

MMP-9 overexpression suppresses the LPS-induced IL-6 secretion in the primary hepatocytes

Given the strong link between LPS challenge and MMP-9-mediated inflammation observed *in vivo*, we next sought to determine whether these effects were directly mediated at the cellular level. Primary hepatocytes were isolated, and their response to LPS stimulation was assessed. We induced MMP-9 overexpression by transfecting the cells with the pCMV6-mMMP-9 plasmid (Fig. 3A). LPS stimulated IL-6 secretion, whereas MMP-9 overexpression decreased the LPS-induced IL-6 secretion (Fig. 3B). These findings offer compelling gain-of-function evidence that reinforces our *in vivo* observations by using a complementary approach.

MMP-9 overexpression mitigates the LPS-induced IL-6 secretion in Hepa1-6 cells

To confirm the protective effects of MMP-9 against hepatic inflammatory responses, a Tet-on (TO) inducible MMP-9 system was established in mouse hepatoma cells. The pLVX-Tet-On-mMMP-9 construct was integrated into Hepa1-6 cells via lentiviral infection. Wild-type Hepa1-6 cells served as the control group because LPS did not stimulate the gene expression of *Mmp9* in Hepa1-6 cells (Fig. S1). After 24-hour doxycycline (Dox) treatment, the enzyme activity MMP-9 in the conditioned medium (Fig. 4A), protein (Fig. 4B), and mRNA (Fig. 4C) expression of MMP-9 in the cell lysates were significantly induced. MMP-9 overexpression significantly reduced IL-6 secretion in hepatocytes after LPS treatment (Fig. 4D). However, MMP-9 overexpression did not alter the mRNA expression of *Il6* and *Tnf* in Hepa1-6 cells following LPS administration (Fig. 4E, F). In summary, these results further support the protective role of MMP-9 against endotoxin challenge in hepatocytes, which appears to be mediated through mechanisms independent of local transcription of pro-inflammatory cytokines.

The hemopexin domain is critical for attenuating LPS-induced IL-6 secretion in hepatocytes

Although MMP-9 has been shown to exert protective effects, the mechanism by which it suppresses LPS-induced IL-6 secretion remains unclear, particularly whether this regulation depends on its enzymatic activity or PEX domain. To address this, we generated two functionally impaired MMP-9 variants: a catalytically inactive mutant (E402A) and a hemopexin domain-deletion form (Δ PEX), as illustrated in Fig. 5A. E402A and Δ PEX variants cloned into doxycycline-inducible pLVX-Tet-On vectors were introduced into Hepa1-6 cells via lentiviral transduction. Zymography was performed using conditioned medium to validate cell line activity. As expected,

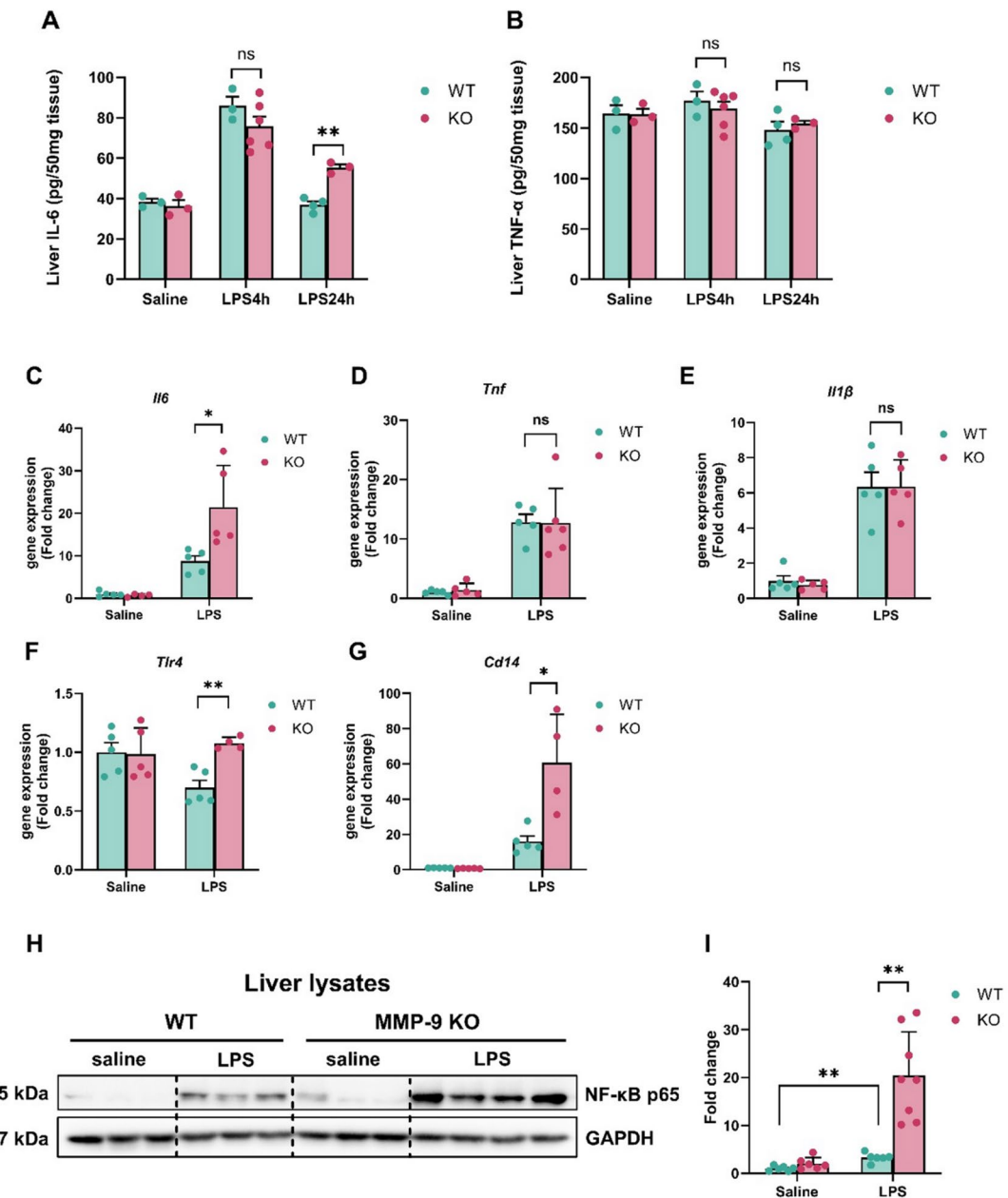


Fig. 2. MMP-9 knockout increases hepatic inflammatory response after LPS administration. (A, B) ELISA quantified protein levels of IL-6 and TNF- α in liver lysates following LPS injection (4.5 mg/kg) for 4 and 24 h in WT and MMP-9 KO mice. (C–E) Hepatic mRNA expression of pro-inflammatory cytokines was measured by quantitative PCR. *Rpl19* served as internal control. (F, G) Hepatic mRNA expression of LPS receptors was assessed by qPCR. *Rpl19* served as internal control. (H, I) NF-κB p65 protein levels in liver tissue were analyzed by immunoblotting and normalized to GAPDH. All LPS treatments were performed for 24 h unless otherwise indicated. Data are expressed as mean \pm SEM ($n=3$ –10 per group). Statistical comparisons were made using unpaired t-tests. * $P<0.05$, ** $P<0.01$ vs. WT + LPS; ns: not significant.

the enzymatic activity of MMP-9 was induced in the overexpressed ΔPEX groups but not in the overexpressed E402A groups after 24-hour Dox treatment (Fig. 5B). WT MMP-9 overexpression served as a positive control, and EGFP overexpression was used as a negative control.

The secretion of IL-6 from TO-E402A and TO-ΔPEX in Hepa1-6 cells was analyzed using ELISA. Notably, similar to the overexpression of WT MMP-9, the overexpression of E402A still reduced LPS-induced IL-6 secretion (Fig. 5C), indicating that the protective effects of MMP-9 were not primarily achieved through its catalytic function. However, overexpression of ΔPEX did not affect LPS-induced IL-6 secretion (Fig. 5D), suggesting that the PEX domain plays a major role in MMP-9's protective effect. Collectively, we demonstrated that MMP-9 exerts anti-inflammatory effects through its PEX domain to reduce LPS-stimulated IL-6 secretion in hepatocytes.

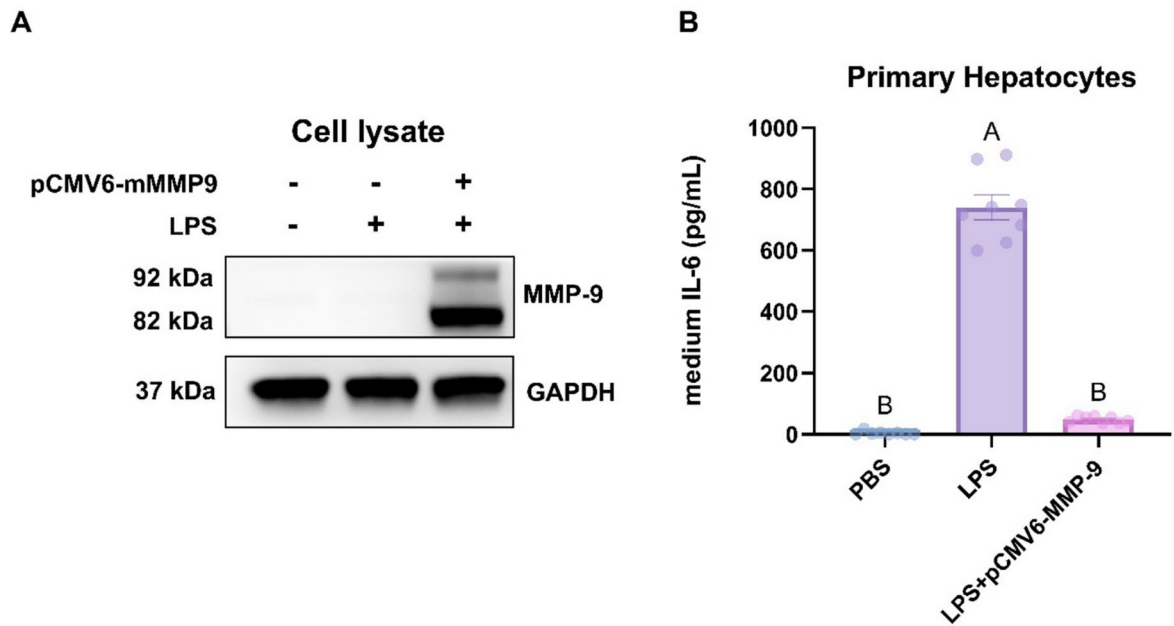


Fig. 3. MMP-9 overexpression decreases IL-6 secretion in primary hepatocytes after LPS induction. Forward transfection of the pCMV6-mMMP-9 plasmid was performed into primary hepatocytes for 24 h, following LPS induction for another 24 h. (A) MMP-9 protein levels in cell lysates were assessed by immunoblotting. GAPDH was used as an internal control. (B) ELISA analyzed the IL-6 secretion in conditioned medium samples. Data are presented as mean \pm SEM. $n=8$. Different letters represent significant differences determined by one-way ANOVA following Turkey's multiple comparison. $p<0.05$.

MMP-9 overexpression attenuates the secretion of LPS-induced IL-6 in RAW264.7 cells

LPS is a well-established inducer of MMP-9 expression in macrophages⁴². In the liver, immune cells, particularly Kupffer cells, serve as a major source of both pro-inflammatory cytokines and MMP-9^{5,43}. Based on this, we hypothesized that Kupffer cells respond to LPS stimulation and actively mediate inflammatory signaling under the regulation of MMP-9. Therefore, we used RAW264.7, a mouse macrophage cell line, to study the role of MMP-9 in the inflammatory response of Kupffer cells. The pLVX-Tet-On-mMMP-9 construct was integrated into RAW264.7 cells through lentiviral infection. After 24-hour Dox treatment, the enzyme activity of MMP-9 in the conditioned medium (Fig. 6A), protein (Fig. 6B), and mRNA (Fig. 6C) expression of MMP-9 in the cell lysates were significantly induced, suggesting successful overexpression. MMP-9 overexpression decreased LPS-induced IL-6 secretion by macrophages (Fig. 6D). However, MMP-9 overexpression did not significantly alter the mRNA expression of *Il6* and *Tnf* in RAW264.7 cells following LPS stimulation, although the expression of *Il6* showed a downward trend (Fig. 6E, F). Similar activation profiles observed in hepatocytes and macrophages demonstrated that MMP-9 exerts a protective effect against LPS-induced inflammation in both hepatocytes and macrophages, suggesting a shared mechanism through which MMP-9 contributes to hepatic immune regulation.

MMP-9 knockout increases LPS-induced IL-6 secretion but not gene levels in RAW264.7 cells

A loss-of-function study was conducted to provide evidence for the role of MMP-9 in LPS-induced inflammation in macrophages using the lentiviral CRISPR/Cas9 approach to disrupt *Mmp9* gene expression. Two guide RNAs targeting MMP-9 #31,583 and #31,592 were constructed in lentiCRISPRv2 plasmids and integrated into RAW264.7 cells by lentiviral infection. To validate MMP-9 knockout efficiency, the cells were stimulated with 100 ng/mL LPS for 24 h, and the conditioned medium was collected for gelatin zymography. The enzymatic activity of MMP-9 was markedly reduced in the cells transduced with gRNA #31,583, whereas this reduction was minimal in the #31,592 group (Fig. 7A). Therefore, we selected #31,583 cells as the model for further experiments. Following LPS stimulation, the mRNA levels of *Il6* and *Tnf* remained comparable between the WT and MMP-9 KO groups, indicating that the transcriptional regulation of these cytokines was not significantly affected by the loss of MMP-9 (Fig. 7B, C). However, LPS-induced IL-6 secretion into the medium was significantly higher in MMP-9 KO macrophages than in WT controls (Fig. 7D), suggesting that MMP-9 post-transcriptionally regulated IL-6 levels.

Discussions

This study identified MMP-9 as a novel regulator of hepatic inflammation, primarily through modulation of IL-6 secretion via its PEX domain. Our *in vivo* and *ex vivo* findings confirmed that MMP-9 protein expression is a key factor in the regulation of hepatic inflammatory response. In addition, *in vitro* findings demonstrated that the PEX domain is critical for attenuating IL-6 release in hepatocytes and macrophages under LPS stimulation, suggesting a domain-specific anti-inflammatory role for MMP-9.

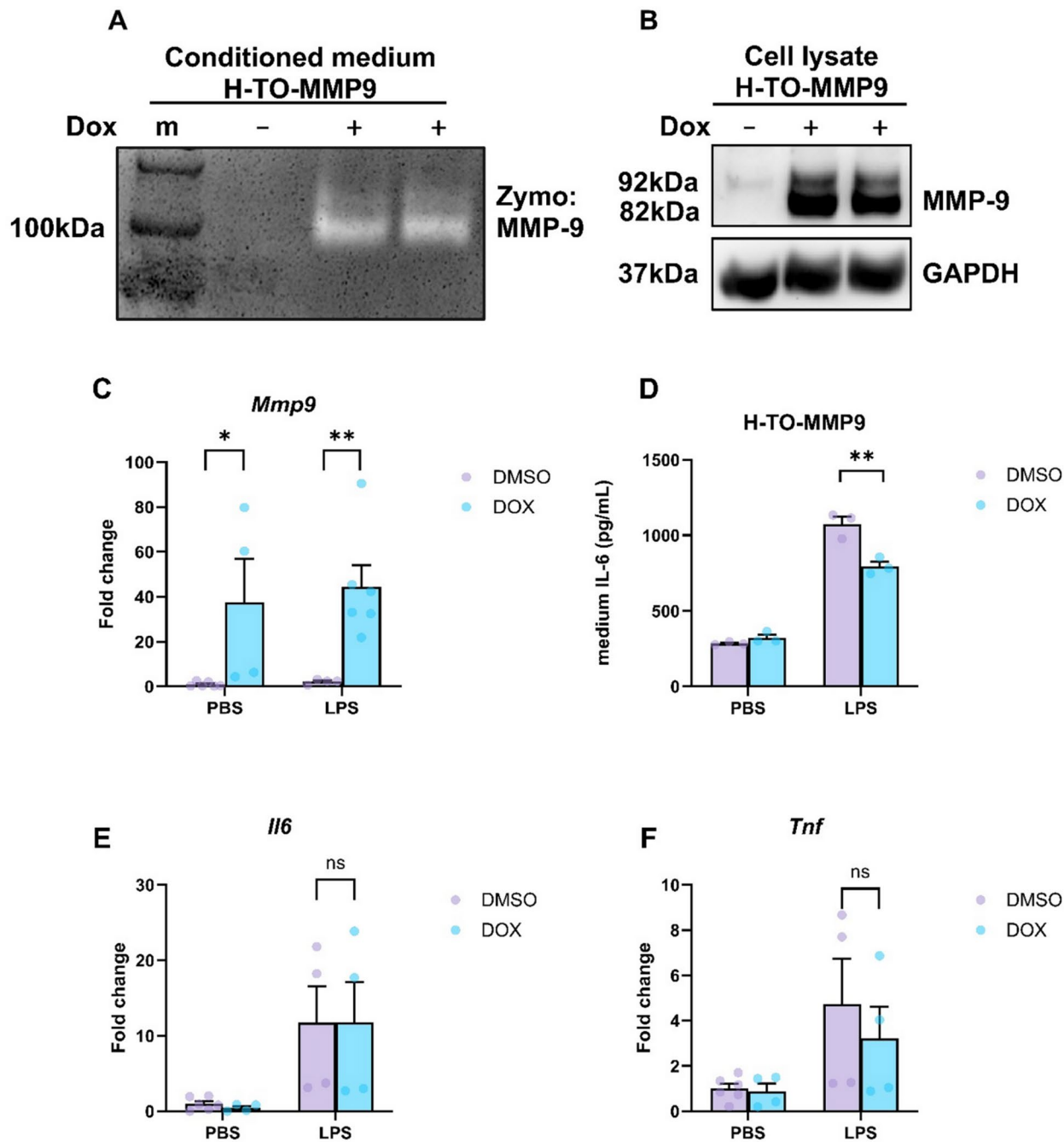
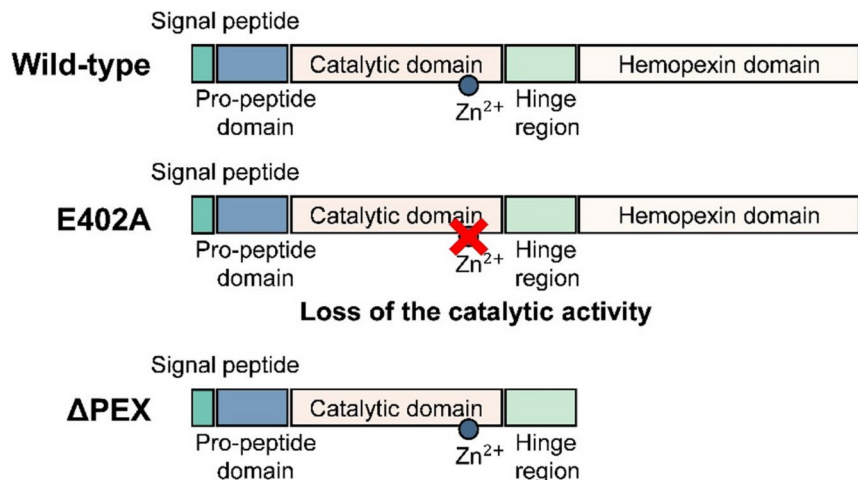


Fig. 4. Inducible MMP-9 expression reduces LPS-induced IL-6 secretion in Hepa1-6 cells without affecting *Il6* mRNA levels. Hepa1-6 cells were transduced with a doxycycline (Dox)-inducible MMP-9 expression construct (pLVX-Tet-On-mMMP9). (A) MMP-9 enzymatic activity in the conditioned medium was assessed by zymography following Dox treatment (1 μ g/mL, 24 h). (B) Intracellular MMP-9 protein levels were evaluated by immunoblotting. (C–F) Cells were co-treated with 24-hour Dox (1 μ g/mL) and 8-hour LPS (100 ng/mL). The mRNA levels of *Mmp9*, *Il6*, and *Tnf* were measured by qPCR. *Rpl19* was used as a housekeeping gene. (D) Secreted IL-6 levels in the conditioned medium were measured by ELISA following 24-hour co-treatment with Dox and LPS stimulation. Data are presented as mean \pm SEM ($n=3$ –6 per group). Statistical comparisons were performed using unpaired t-tests. * $P<0.05$, ** $P<0.01$ vs. control; ns: not significant. m: marker.

In LPS-challenged mice, MMP-9 deficiency led to a significant increase in IL-6 levels. However, TNF- α levels remained unchanged after 4 h of LPS treatment, suggesting a differential regulatory mechanism among pro-inflammatory cytokines, consistent with a previous study demonstrating interactive signaling pathways governing IL-6 and TNF- α expression, mediated via the p38 MAPK and ERK1/2 activation pathways in neonatal and adult whole blood at different LPS dosages⁴⁴. Such divergent responses support the hypothesis in this study that MMP-9 appears to function as a selective modulator of IL-6 during the acute LPS response. Subsequently,

A Different types of MMP-9 constructs



B

Conditioned medium

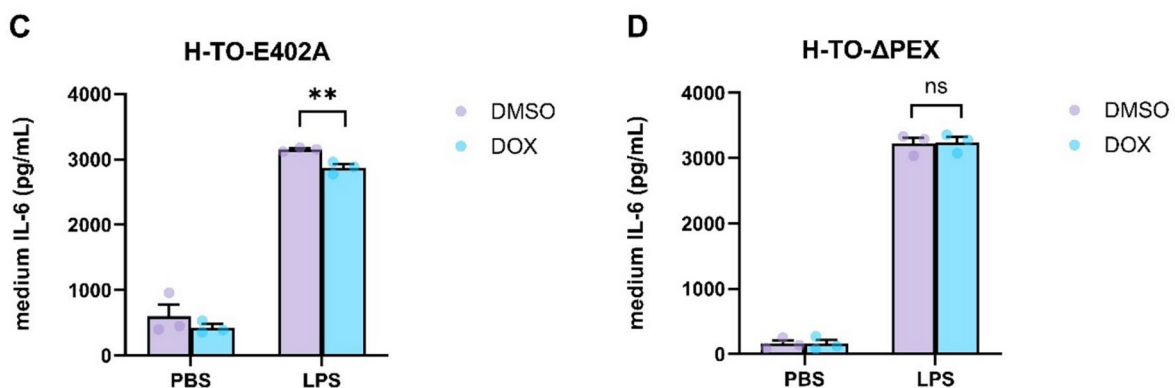
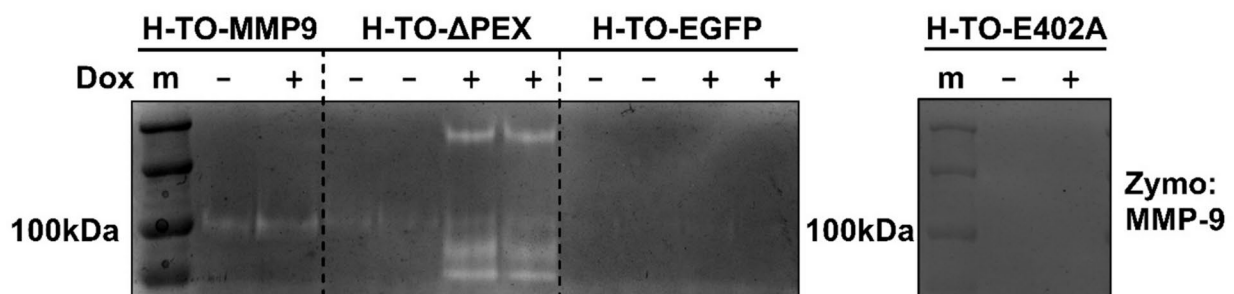


Fig. 5. Hemopexin domain deletion of MMP-9 fails to suppress LPS-induced IL-6 secretion in Hepa1-6 cells. Hepa1-6 cells were transduced with doxycycline (Dox)-inducible lentiviral constructs encoding Δ PEX, E402A variants of MMP-9, or EGFP control. (A) Schematic diagram illustrating domain structures of mutant MMP-9 constructs. (B) MMP-9 enzymatic activity in the conditioned medium was assessed by zymography following Dox treatment (1 μ g/mL for 24 h). (C, D) ELISA measured IL-6 secretion in conditioned medium from Δ PEX and E402A mutant cell lines co-treated with Dox and LPS (100 ng/mL) for 24 h. Data are presented as mean \pm SEM ($n=3$ per group). Statistical comparisons were performed using unpaired t-tests. * $P<0.05$, ** $P<0.01$ vs. DMSO control; ns: not significant. m: marker.

it may adopt a broader suppressive role, contributing to the later regulation of other inflammatory cytokines. Additionally, MMP-9 overexpression in primary hepatocytes significantly decreased IL-6 secretion, confirming its specific role in the suppression of IL-6.

Although the anti-inflammatory potential of MMP-9 has been previously suggested, the underlying mechanisms remain undefined^{32,33}. The results of E402A and Δ PEX in hep1-6 cells implicate the PEX

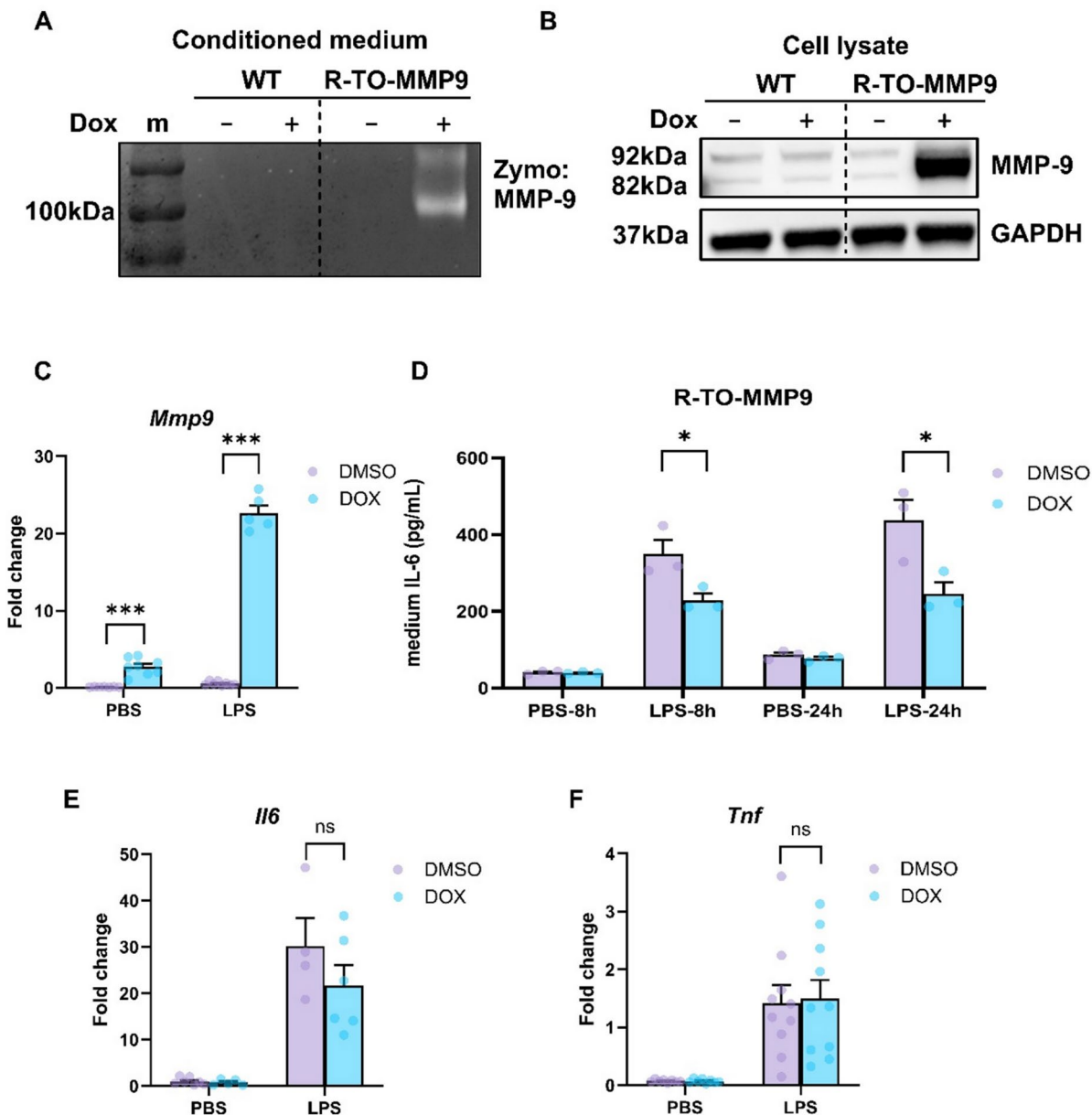


Fig. 6. Inducible MMP-9 expression reduces LPS-induced IL-6 secretion in RAW264.7 cells without affecting *Il6* mRNA levels. RAW264.7 cells were transduced with a doxycycline (Dox)-inducible MMP-9 expression vector (pLVX-Tet-On-mMMP-9). (A) MMP-9 enzymatic activity in the conditioned medium was assessed by zymography following Dox induction (1 μ g/mL for 24 h). (B) Intracellular MMP-9 protein levels were evaluated by immunoblotting. (C–F) Cells were either co-treated with Dox and LPS (100 ng/mL) for 24 h or pretreated with Dox for 16 h prior to LPS stimulation. Gene expression levels of *Mmp9*, *Il6*, and *Tnf* were measured by quantitative PCR using *Rpl19* as internal control. (D) ELISA determined IL-6 secretions in conditioned medium. Data are presented as mean \pm SEM ($n=3$ –6 per group). Statistical analyses were performed using unpaired t-tests. * $P<0.05$, ** $P<0.01$ vs. control; ns: not significant. m: marker.

domain as a functional interface through which MMP-9 interacts with inflammatory signaling components. Mechanistically, the PEX domain has been implicated in protein-protein interactions involved in receptor-mediated internalization and signaling, notably through LRP-1 and TIMP-1 binding^{45,46}. Prior studies have suggested that this interaction contributes to the downstream modulation of ERK1/2 and Akt phosphorylation, potentially altering inflammatory cell behavior²⁷. However, the precise downstream effectors that interact with the PEX domain in the hepatocytes and macrophages remain unknown. Notably, MMP-9 overexpression reduced IL-6 protein secretion without affecting *Il6* mRNA expression, indicating a post-transcriptional regulatory effect. This observation aligns with reports demonstrating a temporal dissociation between IL-6 transcription and protein secretion in LPS-treated monocytes and fibroblasts, suggesting that MMP-9 may regulate IL-6 at the translational or secretion level⁴⁷. Moreover, the findings of gain- and loss-of-function in RAW264.7 suggest

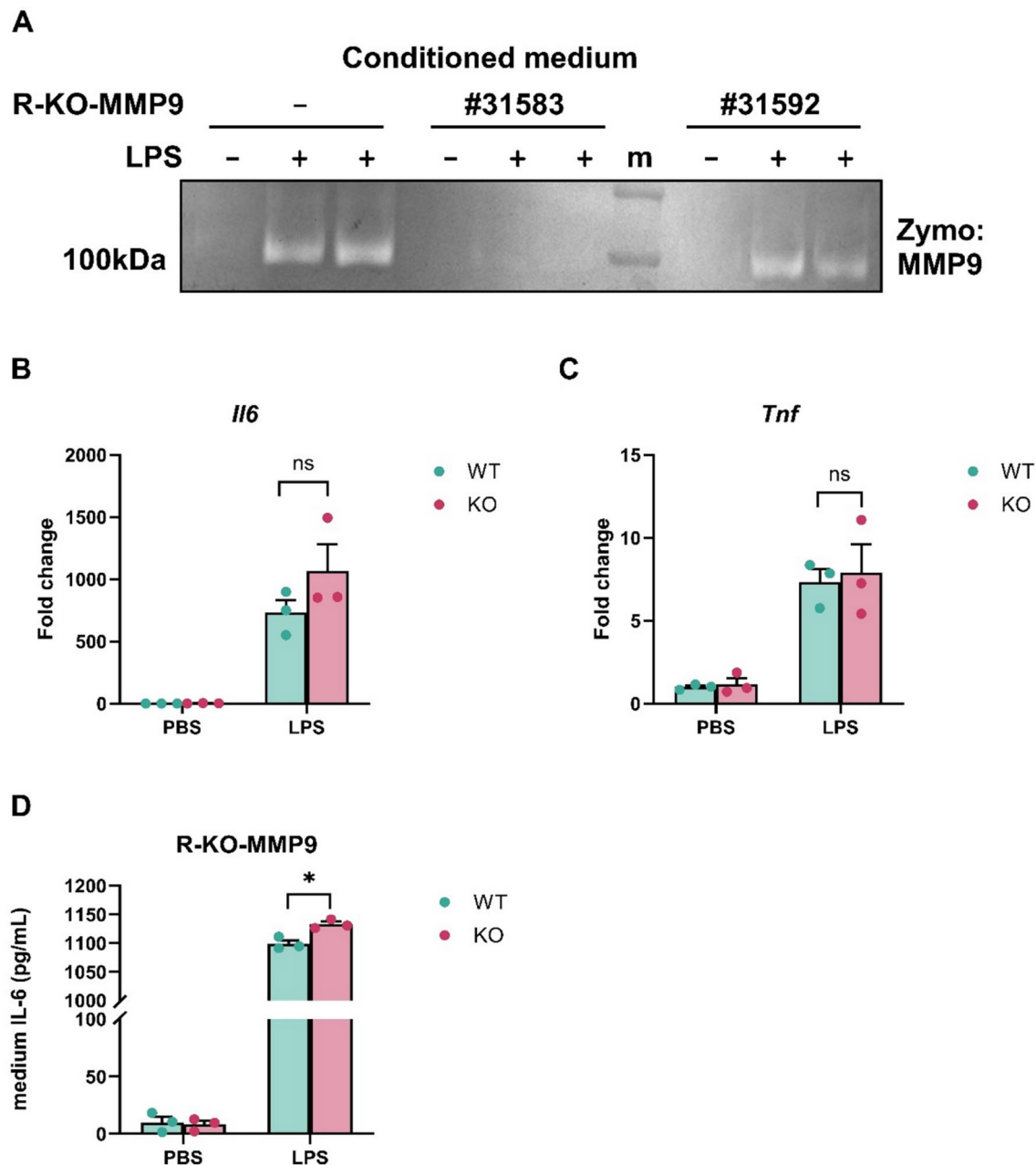


Fig. 7. MMP-9 deficiency enhances LPS-induced IL-6 secretion in RAW264.7 macrophages. RAW264.7 cells were transduced with lentiCRISPRv2 vectors encoding MMP-9-targeting guide RNAs to generate MMP-9 knockout cell lines. Cells were treated with LPS (100 ng/mL) for 24 h. (A) MMP-9 enzymatic activity in the conditioned medium was evaluated by zymography. WT cells treated with PBS served as a negative control; WT cells treated with LPS served as a positive control. (B, C) mRNA levels of *Il6* and *Tnf* were assessed by quantitative PCR from cell lysates, using *Rpl19* as an internal control. (D) Secreted IL-6 protein levels in the conditioned medium were quantified by ELISA. Data are expressed as mean \pm SEM ($n=3-4$ per group). Statistical comparisons were made using unpaired t-tests against LPS-treated WT controls. ns: not significant. m: marker.

that both hepatocytes and macrophages in the liver are responsive to MMP-9 signaling and participate in its anti-inflammatory effects.

We observed similar protective effects of MMP-9 on IL-6 protein expression *in vivo* and *in vitro*. However, the discrepancy in *Il6* gene expression likely reflects key physiological differences between whole organisms and isolated cell cultures. In the liver tissue, *Il6* gene levels were markedly upregulated in MMP-9 KO groups, but this was not observed in hepatocytes or macrophage cell lines, possibly because of the absence of systemic factors *in vitro*. Systemic inflammation, which is activated by complex immune and hormonal networks *in vivo*, has not been fully reproduced in isolated cultures. Additionally, the absence of MMP-9 may impair LPS clearance,

as we only observed an increase in the *Il6* gene in the liver at 24 h post-LPS exposure. *In vitro* systems lack the full spectrum of cell-cell interactions and immune components, likely leading to minimal transcriptional responses. For instance, under LPS stimulation, Kupffer cells and macrophages produce both MMP-9 and pro-inflammatory cytokines, whereas hepatocytes primarily secrete cytokines with minimal MMP-9 expression¹⁰. Hepatocytes may be protected by MMP-9 and affected by the cytokines secreted by Kupffer cells. Moreover, while the protective effect of MMP-9 catalytic activity was not observed *in vitro*, we cannot exclude the possibility that its catalytic function contributes to hepatic inflammatory protection *in vivo* through indirect systemic effects or cellular communication within the liver.

This study has other limitations and potential directions for future research. First, neutrophils constitute only a minor population within the liver, while expressing high levels of *Mmp9*, and can exert both pro- and anti-inflammatory functions during sepsis-associated hepatic injury⁴⁸. In this study, we focused on resident macrophages and hepatocytes, which have less *Mmp9* expression but comprise the major cell types in the liver; nevertheless, the potential role of neutrophils under LPS administration can be further developed. Second, the exact molecular partners of the PEX domain have not been identified, and functional *in vivo* validation of PEX-specific interventions remains to be explored. At the same time, IL-6 suppression was demonstrated; whether PEX-mediated signaling affects other inflammatory mediators warrants further investigation. Third, our study focused on acute LPS-induced inflammation; however, the role of MMP-9 in chronic inflammatory conditions remains unclear. Chronic LPS exposure, as observed in metabolic disorders and liver fibrosis⁴⁹, may engage distinct compensatory mechanisms or alter the balance between MMP-9, MMP-2, and TIMP-1. Investigating MMP-9's role in models of prolonged inflammation or liver injury, such as non-alcoholic steatohepatitis (NASH) or liver fibrosis, could provide a broader understanding of its physiological relevance. Additionally, MMP-9 may play distinct roles at different stages of the inflammatory response. A time-course study of LPS injections in MMP-9 KO mice could help delineate the temporal dynamics of the involvement of MMP-9 in inflammation and tissue remodeling.

In conclusion, our findings identify the PEX domain of MMP-9 as a key suppressor of hepatic IL-6 secretion under inflammatory stress, offering a potential therapeutic target for modulating hepatic inflammation. Although this study was conducted in mice and mouse cell models, the cellular sources and regulatory mechanisms of MMP-9 are highly conserved across mammalian species. Clinical studies have reported the liver's role in the response to LPS⁵⁰ and have demonstrated an association between sepsis and the TIMP-1/MMP-9 ratio⁵¹. Therefore, our findings in mice may provide mechanistic insights relevant to human liver inflammation, although direct relevance to humans requires further validation. Future studies are needed to characterize the interacting proteins and downstream pathways responsible for PEX-mediated immunomodulation and to assess the translational potential of PEX-based anti-inflammatory therapies in acute liver diseases.

Methods

Animals and treatments

C57BL/6 wild-type mice (Laboratory Animal Center of National Taiwan University) and B6.FVB(Cg)-MMP-9_{tm1Tvu/J} (MMP-9^{-/-}, KO) mice (Jackson Laboratory) (10–15 weeks old, 19–27 g) were used in this study. The experimental animals were raised under a 12-hour light to 12-hour darkness cycle at 25±2 °C and approximately 50% humidity, with a chow diet and water ad libitum. Nineteen male mice were weighed and utilized after intraperitoneal injection of saline or 4.5 mg/kg LPS (Sigma) for 24 h, and liver and plasma samples were collected for ELISA, immunoblotting, and real-time PCR. Euthanasia was conducted using CO₂ inhalation as the primary method, delivered from a compressed gas cylinder into a non-stressful chamber at a fill rate of 30–70% displacement of the chamber volume per minute. To ensure complete death, cervical dislocation was subsequently performed as a secondary physical method, in accordance with the institution's IACUC-approved protocol for the Euthanasia of Animals. Animal management followed the "Administrative Regulations for Laboratory Animal Houses of the National Taiwan University Campus." The study is reported in accordance with ARRIVE guidelines.

Blood biochemistry

Blood samples were collected from the orbital sinus using heparinized microhematocrit tubes (80 IU/mL) for plasma biochemistry analysis. The samples were centrifuged at 7,000 × g for 10 min at room temperature to separate plasma. Plasma biochemical parameters, including lactate dehydrogenase, alanine aminotransferase, aspartate aminotransferase, and albumin, were quantified using a Spotchem SP-4410 biochemical analyzer (Arkray) along with the corresponding reagent test strips.

Histological study

Liver tissues were fixed in 10% neutral-buffered formalin for 16 h, followed by standard paraffin embedding and dehydrated using graded ethanol, cleared in xylene, and infiltrated with paraffin before being embedded in molds. Section (5 µm) were cut using a microtome, floated in 42 °C water, and mounted onto glass slides. For H&E staining, sections were deparaffinized, rehydrated, stained with hematoxylin and eosin, dehydrated, and mounted. For immunohistochemistry (IHC), antigen retrieval was performed in boiled citrate buffer (10 mM sodium citrate, 0.05% Tween-20, pH 6.0). Endogenous peroxidase activity was blocked with hydrogen peroxide, followed by blocking with 3% normal goat serum. Slides were incubated with primary antibodies at 4 °C overnight, and detection was performed using a Rabbit-Specific HRP/DAB Detection Kit (Abcam). The antibodies used in this study are provided in Supplementary Table 4. Counterstaining was performed with hematoxylin. The F4/80-positive areas were quantified using the ImageJ software from at least three non-overlapping fields per sample and three biological replicates per group.

ELISA

According to the manufacturer's instructions, the enzyme-linked immunosorbent assay for the quantitative detection of mouse cytokines was performed using the IL-6 Mouse ELISA Kit (Invitrogen) and TNF- α Mouse ELISA Kit (Invitrogen). The concentration of homogenized liver tissue was standardized to 500 mg/mL in radioimmunoprecipitation assay (RIPA) lysis buffer (Thermo Fisher) with PhosSTOP (Roche) and EDTA-free Protease Inhibitor Cocktail (Roche). Conditioned medium samples from *in vitro* studies were harvested and stored at -80 °C.

RNA extraction and RT-PCR analysis

Total RNA was extracted from tissues and cells using GENEzol reagent (Geneaid). Tissues (40 mg) were homogenized for 20 min in 0.5 mL GENEzol with beads, then centrifuged at 13,000 \times g for 10 min at 4 °C to collect the supernatant. Cells were lysed in 1 mL GENEzol for 5 min. Each 1 mL sample was mixed with 0.2 mL chloroform, incubated at room temperature for 3 min, and centrifuged at 13,000 \times g for 15 min at 4 °C. The upper aqueous phase (0.5 mL) was mixed with 0.5 mL isopropanol, incubated on ice for 10 min, and centrifuged at 13,000 \times g for 10 min at 4 °C. RNA pellets were washed twice with 75% ethanol, air-dried for 5 min, and dissolved in DEPC water.

cDNA was synthesized using the PrimeScript™ RT Reagent Kit (Takara), following the manufacturer's instructions. QuantStudio 3 Real-Time PCR System (Thermo Fisher) was used for qPCR. Each 10 μ L reaction contained 5 μ L PowerUp™ SYBR™ Green Master Mix (Applied Biosystems), 0.4 μ L primer mix (10 μ M each), and 2 μ L cDNA. The cycling conditions were: 50 °C for 2 min, 95 °C for 2 min, followed by 40 cycles of 95 °C for 1 s and 60 °C for 30 s. Data were analyzed using Design and Analysis Software 2.6.0. Primer sequences are listed in Supplementary Table 5.

Primary hepatocyte

Mouse primary hepatocytes were isolated by a modified two-step collagenase perfusion method. Perfusion Medium I (PBS added with 10 mM HEPES, 0.5 M Glucose, 0.2 mM EDTA), Perfusion Medium II (PBS added with 30 mM HEPES, 0.5 M Glucose, 1 mM CaCl₂), and Collagenase Solution (collagenase type I, DNase I, and BSA in Perfusion Medium II) were pre-warmed to 37 °C prior to use. Male C57BL/6 mice (9–10 weeks old) were anesthetized, and abdominal incisions were made. The portal vein was cannulated with a 27-G butterfly needle, and the liver was perfused via the portal vein with \geq 10 mL of perfusion medium I, followed by \geq 10 mL of Collagenase Solution. The liver was excised after perfusion.

The cell suspension was filtered through a 150 μ m mesh and placed on ice. An equal volume of cold culture DMEM medium (Merck, D5030) with 10% FBS was added, and the suspension was centrifuged at 50 \times g for 5 min at 4 °C. The pellet was washed with Perfusion Medium II and centrifuged again under identical conditions. Red blood cells were lysed using RBC lysis buffer (1 min, 50 \times g, 4 °C), followed by a final wash with Perfusion Medium II. The hepatocyte pellet was resuspended in pre-warmed culture medium and passed through a 70 μ m strainer, and seeded in 24-well plates. The following day, the cells were refreshed with culture medium and transfected with the pCMV6-mMMP9 plasmid. Twenty-four hours post-transfection, the medium was refreshed again, and the cells were treated with LPS for 24 h, as indicated.

Cell culture and stimulation

RAW264.7, a *Mus musculus* macrophage cell line (ATCC® TIB-71™), Hepa1-6, a *Mus musculus* hepatocyte cell line (ATCC® CRL-1830™), and 293T, a *Homo sapiens* embryonic kidney cell line (ATCC® CRL-3216™), were cultured in DMEM with high glucose medium (Gibco) supplemented with 10% fetal bovine serum, 1% Penicillin-Streptomycin, 3.7 mg/L NaHCO₃, and 1 mM sodium pyruvate and disinfected with a 0.22 μ m filter. The Cells were maintained at 37 °C, 90% relative humidity, and 5% CO₂. Numerous cell lines were artificially engineered to perform loss- and gain-of-function experiments, as outlined in Supplementary Table 2.

Production of lentivirus and cell infection with selection

The lentivirus was produced in 293T cells using Lipofectamine 3000 Transfection Reagent (Thermo Fisher Scientific) according to the manufacturer's instructions. The transfected plasmids included the packaging plasmids pMD2.G (a gift from Didier Trono; Addgene plasmid # 12259; <http://n2t.net/addgene:12259>; RRID: Addgene_12259), psPAX2 (a gift from Didier Trono; Addgene plasmid # 12260; <http://n2t.net/addgene:12260>; RRID: Addgene_12260), pAdVAntage (Promega), and the lentiviral expression plasmid at a ratio of 1:1.8:0.6:3. Lentiviral supernatant was collected 48 h after transfection using a 0.45 μ m filter and stored at -20 °C. Hepa1-6 and RAW264.7 cells were infected with a serial dilution of lentivirus for 24 h, and then replaced with the culture medium for another 24 h. The infected RAW264.7 cells were selected with 5 μ g/mL puromycin and Hepa1-6 cells with 15 μ g/mL puromycin for 48 h. The 20–30% cell survival groups were maintained.

CRISPR gRNA target design and cloning

CRISPR gRNAs were designed using the Zhang Lab online platform (crispr.mit.edu) to knockout MMP-9 in RAW264.7 cells^{52,53}. Two specific MMP-9 gRNA targets, #31,583 and #31,592, were selected (Supplementary Table 3). Forward and reverse oligos (100 μ M each) were annealed in buffer with 50 mM HEPES and 100 nM NaCl by gradually reducing the temperature from 94 °C to 37 °C. The lentiCRISPRv2 plasmid (a gift from Feng Zhang, Addgene plasmid # 52961; <http://n2t.net/addgene:52961>; RRID: Addgene_52961) was linearized using BsmBI-BsmBI, and ligated with the annealed gRNAs using T7 DNA ligase (NEB), following the manufacturer's instructions.

To generate pLVX-Tet-On-mMMP-9, pLVX-Tet-On-E402A-mMMP-9, and pLVX-Tet-On- Δ PEX-mMMP-9 plasmids, the backbone was constructed using the BamHI-EcoRI-linearized pLVX-TetOne-Puro-hAXL vector (a

gift from Kenneth Pienta, Addgene plasmid #124797; <http://n2t.net/addgene:124797>; RRID: Addgene_124797). The E402A mutant was created by substituting glutamate at position 402 with alanine, abolishing enzymatic activity, while the Δ PEX variant lacked the entire PEX domain. Full-length MMP-9, Δ PEX, and E402A fragments were PCR-amplified from the pCMV6-mMMP-9 template using specific primers and Q5 High-Fidelity DNA Polymerase (NEB). The products were subsequently purified using the HiYield Gel/PCR DNA Fragments Extraction Kit 2.0 (Biotech). Ligation was performed with the NEB Gibson Assembly Kit at 50 °C for 1 h using a 1:2 vector-to-insert ratio.

Immunoblot and zymography

Immunoblotting was performed as previously described⁵⁴. The ChemiDoc Touch Imaging system was used to expose the photographs, followed by quantification using Image Lab software. The antibodies used in this study are provided in Supplementary Table 4.

Zymography was performed to determine gelatinase enzyme activity. The 7.5% homemade polyacrylamide gel was embedded with 1.7 mg/mL of gelatin. Culture medium was mixed 1:1 with zymogen buffer solution (4% SDS, 20% glycerol, 0.01% bromophenol blue, and 125 mM Tris-HCl). After electrophoresis, the gel was washed twice for 30 min with washing buffer (2.5% Triton-X100, 50 mM Tris-HCl, 5 mM CaCl_2 , and 1 μM ZnCl_2) and rinsed with deionized water. Gels were incubated overnight at 37 °C in reaction buffer (1% Triton-X100, 50 mM Tris-HCl, 5 mM CaCl_2 , and 1 μM ZnCl_2). After incubation, gels were stained with SimplyBlue™SafeStain (Invitrogen) for 1 h, destained with deionized water for 2 h, and imaged using a ChemiDoc system.

Statistical analysis

In this study, statistical analysis was performed using Prism (GraphPad). *In vivo* data ($n=3$ –10), *ex vivo* data ($n=8$), and *in vitro* data from at least three independent experiments are presented as mean \pm standard error of the mean (SEM). Significant differences ($P<0.05$) were determined using unpaired t-tests and one-way ANOVA following Turkey's multiple comparison.

Data availability

All the data generated or analyzed during this study are included in this published article (and its Supplementary Information files).

Received: 5 August 2025; Accepted: 9 December 2025

Published online: 20 December 2025

References

1. Alexander, C. & Rietschel, E. T. Bacterial lipopolysaccharides and innate immunity. *J. Endotoxin Res.* **7** (3), 167–202 (2001).
2. Wang, X. & Quinn, P. J. Endotoxins: lipopolysaccharides of gram-negative bacteria. *Subcell. Biochem.* **53**, 3–25 (2010).
3. Cheng, M. L., Nakib, D., Perciani, C. T. & MacParland, S. A. The immune niche of the liver. *Clin. Sci. (Lond.)* **135** (20), 2445–2466 (2021).
4. Liaskou, E., Wilson, D. V. & Oo, Y. H. Innate immune cells in liver inflammation. *Mediators Inflamm.* **2012**, 949157 (2012).
5. Robinson, M. W., Harmon, C. & O'Farrelly, C. Liver immunology and its role in inflammation and homeostasis. *Cell. Mol. Immunol.* **13** (3), 267–276 (2016).
6. Nguyen-Lefebvre, A. T. & Horuzsko, A. Kupffer cell metabolism and function. *J. Enzymol. Metab.* **1**, 1 (2015).
7. Mantovani, A. & Garlanda, C. Humoral innate immunity and acute-phase proteins. *N Engl. J. Med.* **388** (5), 439–452 (2023).
8. Wen, Y., Lambrecht, J., Ju, C. & Tacke, F. Hepatic macrophages in liver homeostasis and diseases—diversity, plasticity and therapeutic opportunities. *Cell. Mol. Immunol.* **18** (1), 45–56 (2021).
9. Jia, L. et al. Hepatocyte Toll-like receptor 4 regulates obesity-induced inflammation and insulin resistance. *Nat. Commun.* **5**, 3878 (2014).
10. Norris, C. A. et al. Synthesis of IL-6 by hepatocytes is a normal response to common hepatic stimuli. *PLoS One.* **9** (4), e96053 (2014).
11. Nakamoto, N. & Kanai, T. Role of toll-like receptors in immune activation and tolerance in the liver. *Front. Immunol.* **5**, 221 (2014).
12. MacPhee, P. J., Schmidt, E. E. & Groom, A. C. Evidence for Kupffer cell migration along liver sinusoids, from high-resolution *in vivo* microscopy. *Am. J. Physiol.* **263** (1 Pt 1), G17–23 (1992).
13. Ishibashi, H., Nakamura, M., Komori, A., Migita, K. & Shimoda, S. Liver architecture, cell function, and disease. *Semin Immunopathol.* **31** (3), 399–409 (2009).
14. Li, Y. F. et al. Epigallocatechin-3-Gallate inhibits matrix Metalloproteinase-9 and monocyte chemotactic Protein-1 expression through the 67-kDa laminin receptor and the TLR4/MAPK/NF- κ B signalling pathway in Lipopolysaccharide-Induced macrophages. *Cell. Physiol. Biochem.* **43** (3), 926–936 (2017).
15. Slomiany, B. L. & Slomiany, A. Role of LPS-elicited signaling in triggering gastric mucosal inflammatory responses to *H. pylori*: modulatory effect of Ghrelin. *Inflammopharmacology* **25** (4), 415–429 (2017).
16. Okada, Y. et al. Matrix metalloproteinase 9 (92-kDa gelatinase/type IV collagenase) from HT 1080 human fibrosarcoma cells. Purification and activation of the precursor and enzymic properties. *J. Biol. Chem.* **267** (30), 21712–21719 (1992).
17. Rohani, M. G. & Parks, W. C. Matrix remodeling by MMPs during wound repair. *Matrix Biol.* **44–46**, 113–121 (2015).
18. Castaneda, F. E. et al. Targeted deletion of metalloproteinase 9 attenuates experimental colitis in mice: central role of epithelial-derived MMP. *Gastroenterology* **129** (6), 1991–2008 (2005).
19. Visse, R. & Nagase, H. Matrix metalloproteinases and tissue inhibitors of metalloproteinases: structure, function, and biochemistry. *Circ. Res.* **92** (8), 827–839 (2003).
20. Dufour, A., Zucker, S., Sampson, N. S., Kuscu, C. & Cao, J. Role of matrix metalloproteinase-9 dimers in cell migration: design of inhibitory peptides. *J. Biol. Chem.* **285** (46), 35944–35956 (2010).
21. Yabluchanskiy, A., Ma, Y., Iyer, R. P., Hall, M. E. & Lindsey, M. L. Matrix metalloproteinase-9: many shades of function in cardiovascular disease. *Physiol. (Bethesda)* **28** (6), 391–403 (2013).
22. Van den Steen, P. E. et al. The hemopexin and O-glycosylated domains tune gelatinase B/MMP-9 bioavailability via Inhibition and binding to cargo receptors. *J. Biol. Chem.* **281** (27), 18626–18637 (2006).
23. Ardi, V. C. et al. Neutrophil MMP-9 proenzyme, unencumbered by TIMP-1, undergoes efficient activation *in vivo* and catalytically induces angiogenesis via a basic fibroblast growth factor (FGF-2)/FGFR-2 pathway. *J. Biol. Chem.* **284** (38), 25854–25866 (2009).

24. Xu, J. et al. Role of the SDF-1/CXCR4 axis in the pathogenesis of lung injury and fibrosis. *Am. J. Respir Cell. Mol. Biol.* **37** (3), 291–299 (2007).
25. Ortega, N., Behonick, D. J., Colnot, C., Cooper, D. N. & Werb, Z. Galectin-3 is a downstream regulator of matrix metalloproteinase-9 function during endochondral bone formation. *Mol. Biol. Cell.* **16** (6), 3028–3039 (2005).
26. Alford, V. M. et al. Targeting the Hemopexin-like domain of latent matrix Metalloproteinase-9 (proMMP-9) with a small molecule inhibitor prevents the formation of focal adhesion junctions. *ACS Chem. Biol.* **12** (11), 2788–2803 (2017).
27. Mantuano, E. et al. The hemopexin domain of matrix metalloproteinase-9 activates cell signaling and promotes migration of Schwann cells by binding to low-density lipoprotein receptor-related protein. *J. Neurosci.* **28** (45), 11571–11582 (2008).
28. Aizarani, N. et al. A human liver cell atlas reveals heterogeneity and epithelial progenitors. *Nature* **572** (7768), 199–204 (2019).
29. Bouwens, L., Baekeland, M., De Zanger, R. & Wisse, E. Quantitation, tissue distribution and proliferation kinetics of Kupffer cells in normal rat liver. *Hepatology* **6** (4), 718–722 (1986).
30. MacParland, S. A. et al. Single cell RNA sequencing of human liver reveals distinct intrahepatic macrophage populations. *Nat. Commun.* **9** (1), 4383 (2018).
31. Li, Z. et al. GepLiver: an integrative liver expression atlas spanning developmental stages and liver disease phases. *Sci. Data.* **10** (1), 376 (2023).
32. Moore, B. A., Manthey, C. L., Johnson, D. L. & Bauer, A. J. Matrix metalloproteinase-9 Inhibition reduces inflammation and improves motility in murine models of postoperative ileus. *Gastroenterology* **141** (4), 1283 (2011).
33. Zhang, H. et al. MMP9 protects against LPS-induced inflammation in osteoblasts. *Innate Immun.* **26** (4), 259–269 (2020).
34. McMillan, S. J. et al. Matrix metalloproteinase-9 deficiency results in enhanced allergen-induced airway inflammation. *J. Immunol.* **172** (4), 2586–2594 (2004).
35. Tian, W. & Kyriakides, T. R. Matrix metalloproteinase-9 deficiency leads to prolonged foreign body response in the brain associated with increased IL-1 β levels and leakage of the blood-brain barrier. *Matrix Biol.* **28** (3), 148–159 (2009).
36. Renckens, R. et al. Matrix metalloproteinase-9 deficiency impairs host defense against abdominal sepsis. *J. Immunol.* **176** (6), 3735–3741 (2006).
37. Vu, T. H. et al. MMP-9/gelatinase B is a key regulator of growth plate angiogenesis and apoptosis of hypertrophic chondrocytes. *Cell* **93** (3), 411–422 (1998).
38. Woo, C. H., Lim, J. H. & Kim, J. H. Lipopolysaccharide induces matrix metalloproteinase-9 expression via a mitochondrial reactive oxygen species-p38 kinase-activator protein-1 pathway in Raw 264.7 cells. *J. Immunol.* **173** (11), 6973–6980 (2004).
39. Beutler, B. & Rietschel, E. T. Innate immune sensing and its roots: the story of endotoxin. *Nat. Rev. Immunol.* **3** (2), 169–176 (2003).
40. Masure, S., Proost, P., Van Damme, J. & Opdenakker, G. Purification and identification of 91-kDa neutrophil gelatinase. Release by the activating peptide interleukin-8. *Eur. J. Biochem.* **198** (2), 391–398 (1991).
41. Opdenakker, G., Masure, S., Grillet, B. & Van Damme, J. Cytokine-mediated regulation of human leukocyte gelatinases and role in arthritis. *Lymphokine Cytokine Res.* **10** (4), 317–324 (1991).
42. Yang, C. C. et al. Lipopolysaccharide-Induced matrix Metalloproteinase-9 expression associated with cell migration in rat brain astrocytes. *Int. J. Mol. Sci.* **21**, 1 (2019).
43. Ramachandran, P. et al. Differential Ly-6 C expression identifies the recruited macrophage phenotype, which orchestrates the regression of murine liver fibrosis. *Proc. Natl. Acad. Sci. U.S.A.* **109** (46), E3186–E3195 (2012).
44. Koch, L. et al. LPS- and LTA-induced expression of IL-6 and TNF- α in neonatal and adult blood: role of MAPKs and NF- κ B. *Mediators Inflamm.* **2014**, 283126 (2014).
45. Hahn-Dantona, E., Ruiz, J. F., Bornstein, P. & Strickland, D. K. The low density lipoprotein receptor-related protein modulates levels of matrix metalloproteinase 9 (MMP-9) by mediating its cellular catabolism. *J. Biol. Chem.* **276** (18), 15498–15503 (2001).
46. O'Connell, J. P., Willenbrock, F., Docherty, A. J., Eaton, D. & Murphy, G. Analysis of the role of the COOH-terminal domain in the activation, proteolytic activity, and tissue inhibitor of metalloproteinase interactions of gelatinase B. *J. Biol. Chem.* **269** (21), 14967–14973 (1994).
47. Jin, J. et al. Different signaling mechanisms regulating IL-6 expression by LPS between gingival fibroblasts and mononuclear cells: seeking the common target. *Clin. Immunol.* **143** (2), 188–199 (2012).
48. Fang, L., Song, Y., Chen, J. & Ding, Y. The dual role of neutrophils in sepsis-associated liver injury. *Front. Immunol.* **16**, 1538282 (2025).
49. Cani, P. D. et al. Metabolic endotoxemia initiates obesity and insulin resistance. *Diabetes* **56** (7), 1761–1772 (2007).
50. Jirillo, E. et al. The role of the liver in the response to LPS: experimental and clinical findings. *J. Endotoxin Res.* **8** (5), 319–327 (2002).
51. Lorente, L. et al. Association of sepsis-related mortality with early increase of TIMP-1/MMP-9 ratio. *PLoS One.* **9** (4), e94318 (2014).
52. Shalem, O. et al. Genome-scale CRISPR-Cas9 knockout screening in human cells. *Science* **343** (6166), 84–87 (2014).
53. Sanjana, N. E., Shalem, O. & Zhang, F. Improved vectors and genome-wide libraries for CRISPR screening. *Nat. Methods.* **11** (8), 783–784 (2014).
54. Huang, C. et al. Fatty acids suppress the steroidogenesis of the MA-10 mouse Leydig cell line by downregulating CYP11A1 and inhibiting late-stage autophagy. *Sci. Rep.* **11** (1), 12561 (2021).

Acknowledgements

The authors gratefully acknowledge Dr. I-Hsuan Liu (Department of Animal Science and Technology, National Taiwan University, Taiwan) for providing the pCMV6-mMMP-9 plasmid.

Author contributions

Y.T.C. and Y.H.L. conducted experiments. Y.T.C., Y.H.L., M.C.H., and C.H. conceived of and designed the study. Y.T.C., Y.H.L., and C.H. drafted the manuscript. X.W.C., M.C.H., C.H.C., and C.H. critically revised and edited the manuscript for intellectual content.

Funding

This study was supported by the Ministry of Science and Technology, Taiwan, under Grant Nos. 114-2314-B-002-055 (awarded to Dr. Chien Huang, National Taiwan University) and 109-2314-B-002-099-MY3 (awarded to Dr. Chih-Hsien Chiu, National Taiwan University).

Competing interests

The authors declare no competing interests.

Ethics approval

All animal experiments were approved by the Institutional Animal Care and Use Committee (IACUC) of the National Taiwan University (IACUC Approval No: NTU-111-EL-00139) and were conducted in accordance with the institutional guidelines for animal research.

Additional information

Supplementary Information The online version contains supplementary material available at <https://doi.org/10.1038/s41598-025-32379-y>.

Correspondence and requests for materials should be addressed to C.H.

Reprints and permissions information is available at www.nature.com/reprints.

Publisher's note Springer Nature remains neutral with regard to jurisdictional claims in published maps and institutional affiliations.

Open Access This article is licensed under a Creative Commons Attribution-NonCommercial-NoDerivatives 4.0 International License, which permits any non-commercial use, sharing, distribution and reproduction in any medium or format, as long as you give appropriate credit to the original author(s) and the source, provide a link to the Creative Commons licence, and indicate if you modified the licensed material. You do not have permission under this licence to share adapted material derived from this article or parts of it. The images or other third party material in this article are included in the article's Creative Commons licence, unless indicated otherwise in a credit line to the material. If material is not included in the article's Creative Commons licence and your intended use is not permitted by statutory regulation or exceeds the permitted use, you will need to obtain permission directly from the copyright holder. To view a copy of this licence, visit <http://creativecommons.org/licenses/by-nc-nd/4.0/>.

© The Author(s) 2025